Analysis of Etoposide Binding to Subdomains of Human DNA Topoisomerase IIα in the Absence of DNA†

Didier Leroy, Andrey V. Kajava,‡ Christian Frei,§ and Susan M. Gasser*

Swiss Institute for Experimental Cancer Research (ISREC), CH-1066 Epalinges/Lausanne, Switzerland

Received August 14, 2000; Revised Manuscript Received December 11, 2000

ABSTRACT: Epipodophyllotoxins are effective anti-tumor drugs that inhibit eukaryotic DNA topoisomerase II by trapping the enzyme in a covalent complex with DNA. We show that both the recombinant N-terminal ATPase domain and the B′A′ core domain of human topoisomerase IIα (htopoIIα) bind radiolabeled etoposide specifically, even in the absence of DNA. The addition of ATP impairs etoposide binding to the holoenzyme and the N-terminal domain, but not to the core domain. To see if this interference resembles that between novobiocin and ATP in the bacterial GyrB subunit, we modeled the structure of the N-terminal domain of htopoIIα and performed molecular docking analysis with etoposide. Mutagenesis of critical amino acids, predicted to stabilize the drug within the N-terminal domain, reveals a less efficient binding of etoposide to the mutated proteins as monitored by direct drug binding assays, although the binding of ATP is not affected.

DNA topoisomerase II (topoII)[1] is highly expressed in proliferating cells and has an essential role in the disjunction of sister chromatids (*1*−*3*) and in proper mitotic chromosome condensation (*4*, *5*). These characteristics render this highly conserved nuclear enzyme an effective target for antitumor agents. Clinically relevant topoII inhibitors fall into two general classes, both of which act by trapping the enzyme in a covalent complex with DNA (*6*−*8*). One class intercalates DNA, and apparently impedes the topoII-dependent religation step by altering DNA structure. The other class, which includes the epipodophyllotoxins teniposide and etoposide, has very weak affinity for DNA (*9*) and is thought to prevent the DNA religation step by directly binding the enzyme (*10*). Although etoposide and teniposide are widely used for the treatment of cancers, it is still unclear how these inhibitors bind their target.

The prokaryotic type II topoisomerase gyrase is the target of several bacteriostatic agents including novobiocin, which acts as a competitive inhibitor for ATP hydrolysis (*11*−*14*). Cocrystallization both of the gyrase B (GyrB) N-terminal domain (aa 1−393) with the ATP analogue adenylyl β,γ-imidodiphosphate (ADPNP, *15*) and of a smaller domain (aa 1−220) with novobiocin has provided high-resolution information on how these reagents competitively inhibit the enzyme's activity: both compounds bind in a large cleft in the GyrB N-terminal domain (*16*). Although no crystal structure is available for the eukaryotic ATP binding domain, significant homology exists between the ATPase domain of GyrB and the N-terminal ATPase domain of eukaryotic topoII (*17*; and see below).

Several studies have tried to characterize topoII drug binding sites by selecting for drug-resistant mutants. The results define three widely dispersed clusters of resistance-conferring mutations in the primary structure of the enzyme, yet provide no coherent identification of the drug binding site (*8*, *18*−*25*). One cluster of mutations is found close to the junction between the N-terminal ATPase and the catalytic core domains, a second lies near the active site tyrosine itself, and a third involves the C-terminal domain. These zones of mutation may either contribute to a single drug binding site in the correctly folded enzyme, or be linked to different pathways that regulate the catalytic activity of topoII. Indeed, many indirect mechanisms, including the expression of antisense RNA, promoter mutation, and/or allelic loss, lead to reduced levels of topoII activity and correlate with cellular resistance to topoII inhibitors (reviewed in *26*−*28*).

Here we have taken a biochemical approach to identify the etoposide binding site in human DNA topoisomerase IIα. We characterize the interaction of tritiated etoposide (^{3}H)-VP16 with an N-terminal domain (aa 1−266), as well as with the catalytic core of the enzyme (aa 430−1214, also called B′A′). A spin-column binding technique allows calculation of apparent dissociation constants ranging from 20 to 30 μM for the binding of etoposide to full-length yeast and human enzymes in the absence of DNA. Apparent K_d values of 20 and 9 μM were obtained for the human N-terminal and B′A′ core domains, respectively. ATP was found to displace VP16 from both the full-length enzyme and the N-terminal domain, but not from the catalytic core domain. Using a molecular modeling approach, we examined

† These studies are funded by grants from the Swiss Cancer League, the Swiss National Science Foundation, and the EU BioMED Program to S.M.G.

* Corresponding author. Fax: 41-21-652-6933, tel.: 41-21-692-5886, e-mail: sgasser@eliot.unil.ch.

‡ Current address: Center for Molecular Modeling, CIT, National Institutes of Health, Bethesda, MD 20892-5626.

§ Current address: Fred Hutchinson Cancer Center, Seattle, WA 98109.

[1] Abbreviations: ATP, adenosine 5′-triphosphate; azido(α^{32}P)ATP, 8-azidoadenosine 5′-triphosphate (α^{32}P); CK2β, casein kinase 2 regulatory subunit; topoII, DNA topoisomerase II; GTP, guanosine 5′-triphosphate; GyrB, DNA gyrase B protein; *m*/*o*-AMSA, *m*/*o*-amsacrine; MBP, maltose binding protein; VM26, teniposide; VP16, etoposide.

10.1021/bi0019141 CCC: $20.00
Published on Web 01/19/2001

plausible structures for the N-terminal domain of htopoIIα, based on the crystal structure of GyrB, and simulated the docking of etoposide within the ATP binding pocket. Subsequently, amino acids that were predicted to contact the drug were mutated. We detect a significantly reduced drug binding efficiency of the mutated N-terminal domains, which strongly suggests that etoposide can interact with the ATP pocket of eukaryotic topoII in vitro. Our results are consistent with two models of topoII−etoposide interaction: either sites within the N-terminal and the core domains cooperate to form a single drug binding pocket, or the two sites bind in a mutually exclusive manner and compete for the drug. In either case, the detection of a second drug binding site within topoIIα suggests novel mechanisms for rendering human tumors drug-resistant.

EXPERIMENTAL PROCEDURES

Radiochemicals and Drugs. (^{3}H)VP16 (1.0 Ci/mmol, 1.0 mCi/mL in ethanol) was purchased from Moravek Biochemicals, Inc., Brea, CA. Azido(α^{32}P)ATP (20 Ci/mmol, 2.0 mCi/mL) was purchased from ICN (Costa Mesa, CA). (α^{32}P)ATP (400 Ci/mmol, 10 mCi/mL) was purchased from Amersham. TopoII inhibitors etoposide (VP16), teniposide (VM26), and amsacrines (*m*-AMSA and *o*-AMSA) were obtained from Sandoz Pharma AG (Basel, Switzerland), or as kind gifts of Dr. Y. Pommier (NIH, Bethesda, MD).

Expression and Purification of TopoII and Domains. Wild-type yeast topoII was overexpressed in the *S. cerevisiae* strain GA24 bearing YEpTOP2-PGAL1 (*29*). Full-length human topoIIα was also purified after overexpression in *S. cerevisiae* and was the kind gift of Dr. C. Austin (University of Newcastle, U.K.; see *30*). The enzyme was stored at 0.16 mg/mL in 50 mM Tris-HCl, pH 7.4, 100 mM KCl, and 10% glycerol.

Subfragments of the htopoIIα gene encoding aa 1−266, 1−426, and 1−440 were obtained by PCR from the plasmid YepGALHuTOP2 (*31*) and were fused to the sequence encoding Maltose Binding Protein (MBP; *32*) in pMal C2 (New England BioLabs). The core domain (aa 430−1214 of htopoIIα) was obtained by subcloning the *Mlu*I−*Xho*I fragment from pBabe430−1214 (*33*) and was fused to MBP.

Mutants of htopoIIα$^{1-440}$ were obtained by a two-step PCR procedure (*34*) using YepGALHuTOP2 (10 ng), the 5′ *Mlu*I primer GTCGAACGCGTCCATGGAAGTGTCAC, and a mutated 3′ primer: TATGAGAGCTGG**CCA**ATACATCT-TTTCAAC (V_{137}W), CCTGTCACTTTCTT**AAA**ATCAT-CATCATAG (E_{155}F), CAGGAATACCT**GC**TCCATTAT-TCC (K_{123}A), or TTTGGCTCCATAG**A**CATTTCGACCACC (G_{164}V). PCR reactions were also performed with the 3′ *Xho*I primer CCGCTCGAGTTTGGGAATTCCCTTGATTC and one of the mutated 5′ primers complementary to the mutated 3′ primers described above. After purification, the two PCR products carrying the same mutation were the template for a PCR using the 5′ *Mlu*I and the 3′ *Xho*I primers. Resulting PCR fragments were ligated at the *Mlu*I and *Xho*I sites of pMalC2. All clones were sequenced on both strands. Fusion proteins were induced and purified by standard methods (New England BioLabs). For most assays, the fusion protein MBPhtopoIIα$^{1-440}$ was used; where indicated, a similar protein domain, MBPhtopoIIα$^{1-426}$, was used.

Drug Binding Assays. Highly purified yeast topoII, human topoIIα, or the appropriate fusion proteins (6−10 pmol/assay) were incubated at 22 °C for 10−15 min with a 200-fold excess of (^{3}H)VP16 (1 μCi) in the absence or presence of increasing concentrations of VP16 or ATP in 50 μL of 25 mM Tris-HCl, pH 7.5, 200 mM KCl, 1.0 mg/mL ovalbumin. In control assays, an equivalent volume of the protein storage buffer was used. VP16 was dissolved in 30% ethanol, 3 mg/mL PEG6000, and in all assays, these solvents were added to 3% and 0.3 mg/mL, respectively. Mixtures were loaded on 1 mL columns of Sephadex G-50 fine preequilibrated with the binding assay buffer, columns were centrifuged (Sigma swinging rotor at 1500*g*, 3 min), and bound (^{3}H)VP16 was determined by scintillation counting of the excluded volume, after subtraction of the control values (free ligand recovered in the flow through is <0.1% of the input radioactivity) (*35*). When MBPhtopoIIα fusion domains were used for binding assays, control reactions were performed with equivalent amounts of MBP−CK2*β* (*36*). For each concentration of nonradioactive drug, the specific radioactivity (SR, cpm/pmol) was calculated. The concentration of bound ligand, (B), was obtained by dividing the radioactivity associated to the bound drug by SR. The concentration of free ligand, (F), was calculated after subtraction of (B) from the total concentration of ligand in the assay. (B)/(F) was then plotted as a function of (B) according to Scatchard. A linear regression analysis was performed, and the stoichiometry of binding was determined graphically by the ratio between the amount of VP16 (pmol) at the intersection point of the *x* axis with the plotted line, and the amount of topoisomerase (pmol) used in the assay.

Molecular Modeling. Atomic coordinates of the novobiocin/GyrB complex were kindly provided by Prof. A. Maxwell. VP16 was built using the program TURBO−FRODO (*37*), and its conformational features were analyzed by molecular dynamics simulation and energy minimization using the parameter set CHARMM PARAM19 (*38*) and the program X-PLOR (*39*). Calculations were carried out with the 1/*r*-dependent dielectric constant. VP16 was subjected to a 15 ps molecular dynamics simulation at 300 K and then 1000 steps of conjugate gradient minimization. The initial docking of VP16 in the ATP binding pocket of GyrB was made manually using the program TURBO−FRODO (*37*), and the complex was subjected to energy minimization using X-PLOR (*39*).

The homology modeling of the topoIIα N-terminus 3D structure was performed using the program ICM (*40*), based on the sequence alignment shown in Figure 2A (*17*) with a slight modification introduced in aa 96−100 of htopoIIα. The published htopoIIα sequence was corrected for aa residues I_{109}DPENN_{114} (*31*), and the yeast sequence is from the SwissProt database. The stereoview of the drug binding site was performed with the program MOLSCRIPT (*41*).

Labeling of Topoisomerase II with Azido(^{32}*P)ATP.* Yeast topoII (15 pmol) or the fusion protein MBPhtopo$^{1-266}$ (30 pmol) was incubated at 20 °C for 15 min in the absence or presence of 200 μM VP16. Azido(α^{32}P)ATP (200 pmol) was adjusted in 15 mM Tris-HCl, pH 7.5, 100 mM KCl, 3% ethanol, 0.3 mg/mL PEG6000 (final volume of 40 μL) for 10 min in the dark. After a 10 min irradiation at 330 nm (lamp 8 W), samples were analyzed by 12% SDS−PAGE (*42*). The gel was silver-stained prior to quantification of protein-associated radioactivity by a PhosphoImager.

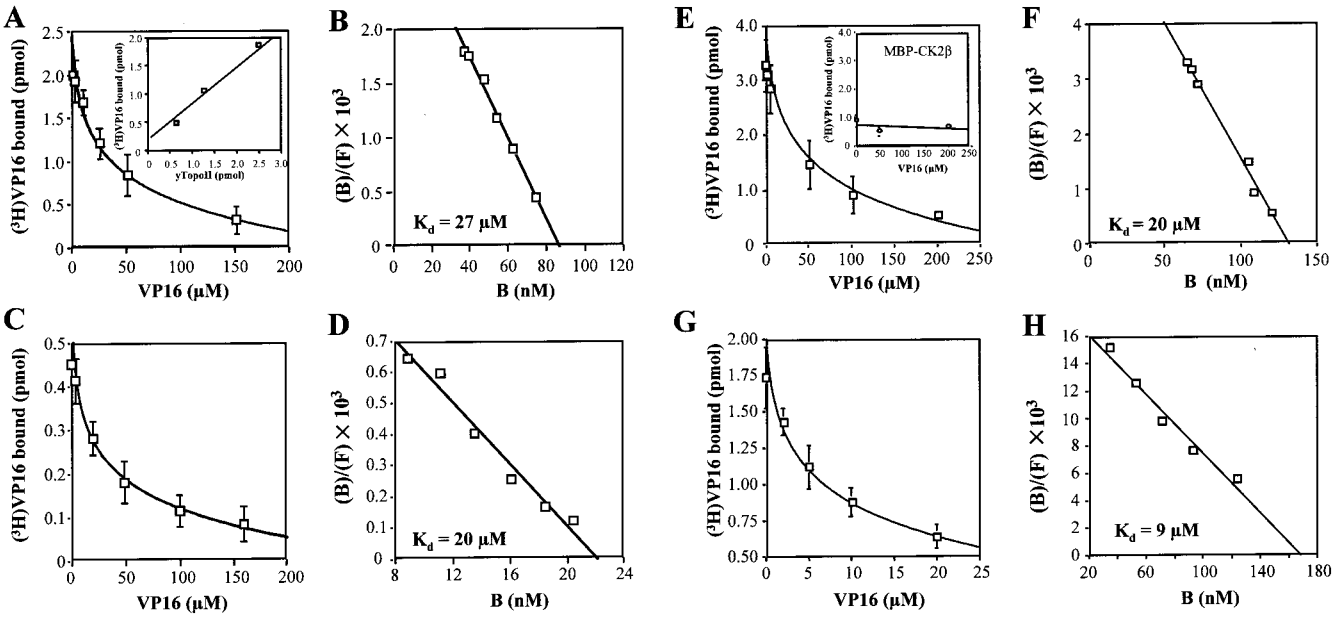

FIGURE 1: Drug binding activity of yeast and human DNA topoII and subdomains. (A) Displacement of (^{3}H)VP16 by unlabeled drug. (^{3}H)VP16 (10^3 pmol, 1.0 μCi) is incubated with 2.5 pmol of yeast topoII in duplicate as described under Experimental Procedures with or without increasing concentrations of unlabeled VP16. Bound and nonbound VP16 are separated by centrifugation over a 1 mL G50 Sephadex column, and the flow-through is counted in scintillation liquid (*35*). Control values (no protein) are subtracted (background is $\leq$0.5 pmol). Inset: 0.65, 1.25, or 2.5 pmol of yeast topoII is incubated with (^{3}H)VP16 (10^3 pmol, 1.0 μCi) as described above. Unlabeled drug can be added before or after the tritiated form with similar results (data not shown). (B) Scatchard plot of the (^{3}H)VP16 displacement shown in panel A. After linear regression calculation, the reciprocal of the slope yields the apparent $K_d = 27$ μM for VP16 and a stoichiometry of 1.6 drug molecules bound per topoII dimer. (B) and (F) stand for the concentrations of bound and free drug molecules, respectively. (C) Displacement of (^{3}H)VP16 by unlabeled drug. (^{3}H)VP16 (400 pmol, 0.4 μCi) is incubated with 0.75 pmol of purified htopoIIα dimer. The drug binding assay is performed in duplicate as in (A), and data are plotted after subtraction of the background ($\leq$0.2 pmol). (D) Scatchard plot of data in panel C. The reciprocal of the slope yields the apparent $K_d = 20$ μM, and a stoichiometry of 1.5 VP16 molecules bound per htopoIIα dimer. (E) Ten picomoles of MBPhtopo$^{1-266}$ is incubated in duplicate with (^{3}H)VP16 (10^3 pmol, 1.0 μCi) with increasing amounts of unlabeled VP16 as in panel A. In the inset, a similar assay performed with MBP$-$CK2β (*36*) leads to nonspecific binding values which are considered as background ($\leq$0.8 pmol) and subtracted from the data. (F) Scatchard plot of data in panel E. The reciprocal of the slope gives an apparent $K_d = 20$ μM and a stoichiometry of 0.7 VP16 molecule bound per MBPhtopo$^{1-266}$. (G) MBPhtopo$^{430-1214}$ (12 pmol) is incubated with (^{3}H)VP16 (500 pmol, 0.5 μCi) as in panel A, and a control assay with MBP$-$CK2β is performed in parallel (not shown). Data from duplicate assays are plotted after subtraction of the background ($\leq$1.2 pmol). (H) Scatchard plot of data in panel G. The reciprocal of the slope gives an apparent $K_d = 9$ μM and a stoichiometry of 0.7 VP16 molecule bound per MBPhtopo$^{430-1214}$.

Analysis of the ATPase Activity. Yeast topoII (0.3 pmol) was incubated at 37 °C for 30 min with (γ^{32}P)ATP (1.0 μCi, 0.5 mM) in the absence or presence of increasing concentrations of VP16 in 50 μL of reaction buffer (50 mM Tris-HCl, pH 7.5, 100 mM KCl, 10 mM $MgCl_2$, 0.5 mM EDTA, 0.5 mM DTT, 30 μg/mL bovine serum albumin). Control assays were performed in the absence of topoII but in the presence of an equivalent volume of the protein storage buffer. ATP hydrolysis was stopped by addition of 750 μL of 8% charcoal previously equilibrated in 250 mM HCl, 2.5 mM $Na_4P_2O_7$, 2.5 mM K_2HPO_4. After a 5 min incubation on ice, tubes were centrifuged at 1500*g* for 5 min at 4 °C. Supernatants were readsorbed on charcoal as described above, and 200 μL was analyzed by liquid scintillation counting. Assays were performed in duplicate.

RESULTS

VP16 Binds Topoisomerase II in the Absence of DNA. To understand the mode of action of antitumor agents and to identify the minimal drug binding domains on topoII, we used a gel-filtration assay which has been previously used to characterize numerous ligand$-$protein interactions (*35*, *43*$-$*45*). This method does not measure an equilibrium binding constant per se, but has allowed the determination of relative dissociation constants for interactions such as β-D-fructose 2,6-bisphosphate with phosphofructokinase (*44*), and GTP with tubulin (*43*). Binding constants determined in this way, for ligands for which the off-rate is relatively slow, are consistent with results obtained by the Hummel$-$Dryer method (*43*).

To confirm that VP16 binds topoII in the absence of DNA, we preincubated increasing amounts of the purified yeast enzyme with (^{3}H)VP16, and separated bound and free ligand by brief centrifugation on ovalbumin-saturated columns. We found a linear increase of (^{3}H)VP16 bound to topoII, as increasing amounts of enzyme are used (Figure 1A, inset). If nonradioactive VP16 is added, a maximal displacement of (^{3}H)VP16 is achieved at 150 μM (Figure 1A). Scatchard plot analysis of the data yields a straight line, suggesting a monophasic affinity system (Figure 1B). The reciprocal of the slope indicates an apparent K_d of 27 μM, with a stoichiometry of binding of 1.6 drug molecules per yeast topoII dimer. Similar binding assays were performed with the human topoIIα, which has an apparent K_d of 20 μM and a stoichiometry of binding of 1.5 drug molecules per htopoIIα dimer (Figure 1C,D). The fact that similar concentrations of these drugs are able to inhibit the ATP-dependent decatenation activity of both human and yeast holoenzymes in vitro underscores the physiological relevance of these binding constants (data not shown).

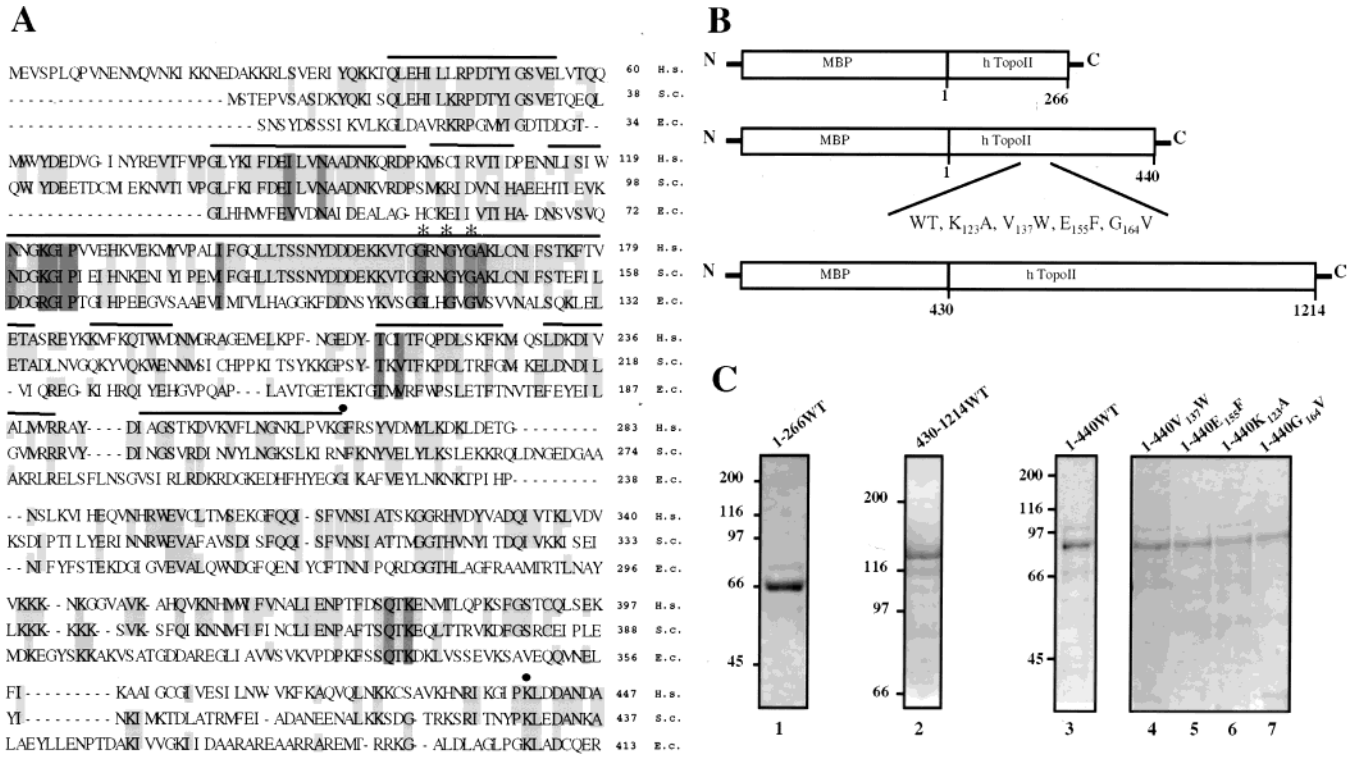

FIGURE 2: Homology between GyrB, human, and yeast topoII ATP binding domains. (A) N-terminal sequence alignments of *Saccharomyces cerevisiae* (S.c.) and human (H.s.) topoII with *E. coli* (E.c.) GyrB (*17*). Light gray shows conserved amino acids, while those important for ATP binding are dark gray. The canonical ATP binding consensus is indicated by asterisks. Points indicate that aa 266 and aa 440 are the C-terminal residues of the htopoIIα domains fused to MBP (see panel B). The sequences used in molecular modeling are indicated by a line. Those not used have lower sequence homology and lie outside the ATP pocket in GyrB. (B) Scheme of the MBP fusion proteins with htopoIIα. Point mutations are Lys_{123}→Ala, Val_{137}→Trp, Glu_{155}→Phe, and Gly_{164}→Val. WT = wild-type. (C) Coomassie blue stained gel of the purified MBP fusion proteins expressed in *E. coli*. Lane 1: MBPhtopo$^{1-266}$WT. Lane 2: MBPhtopo$^{430-1214}$WT. Lane 3: MBPhtopo$^{1-440}$WT. Lanes 4, 5, 6, and 7: MBPhtopo$^{1-440}$ carrying mutations V_{137}W, E_{155}F, K_{123}A, and G_{164}V, respectively.

Subdomains of HtopoIIα Bind Etoposide. To determine which subdomains of topoII are sufficient to bind VP16, we expressed and purified several structural domains of htopoIIα, based on previous analyses of conserved regions (*17*, *46*), and the established crystallization data of GyrB and yeast topoII (*15*, *16*, *47*). As shown in Figure 2A, significant identity exists among the first 450 residues of bacterial, yeast, and human enzymes (*17*). Shading indicates the amino acids of the ATP binding pocket that are most highly conserved from bacteria to man, including the glycines at aa 161, 164, and 166, which define the Walker motif for ATP coordination (see asterisks, Figure 2A). Two htopoIIα domains, one of 266 aa that corresponds to the region of GyrB cocrystallized with novobiocin (*16*) and a second of 440 aa that corresponds to the GyrB fragment cocrystallized with AD-PNP (*15*), were fused to the bacterial Maltose Binding Protein (MBP) and purified to homogeneity (Figure 2C). Because in vitro studies have shown that an N-terminally truncated version of topoII can form a drug-stabilized cleavable complex with teniposide (*48*), we also expressed the central core of htopoIIα fused to MBP (aa 430−1214 or B′A′, based on alignment with gyrase; Figure 2C, lane 2). This corresponds to the core domain of yeast topoII, for which the crystal structure was recently solved (aa 410−1202; *47*).

The binding assay using (^{3}H)VP16 and MBPhtopo$^{1-266}$ was repeated as described above and resulted in a dose-dependent displacement curve that reaches a plateau at 200 μM VP16. Equimolar amounts of MBP−CK2β bind only a background level of (^{3}H)VP16 (0.8 pmol) irrespective of the concentration of unlabeled drug (Figure 1E, inset). This background of nonspecific binding was determined for each assay and was subtracted from other experimental values. The Scatchard plot of data again reveals monophasic displacement kinetics with an apparent K_d of 20 μM, similar to those of full-length yeast and human enzymes (Figure 1F). Analogous results were also obtained for MBPhtopo$^{1-440}$ (see below, Figure 5C).

To see whether the B′A′ core domain also binds the drug in an autonomous manner, we analyzed the binding efficiency of (^{3}H)VP16 to MBPhtopo$^{430-1214}$ as described above, using MBP−CK2β as control. Scatchard analysis of (^{3}H)VP16 displacement results in an apparent K_d of 9 μM and a stoichiometry of 1.4 VP16 molecules bound per B′A′ dimer (Figure 1G,H). In conclusion, both the N-terminal and the core domains of htopoIIα are able to bind VP16 in the absence of DNA. Data from DNA cleavage studies (*48*) are consistent with our demonstration that epipodophyllotoxins bind the catalytic core. Although Olland and Wang (*49*) have recently shown that another topoII inhibitor, ICRF-193, can interact with the N-terminal 400 aa of yeast topoII, ours is the first report suggesting that epipodophyllotoxins can bind the same domain.

ATP and VP16 Compete for Interaction with TopoII and the N-Terminal Subdomain. Since one of the drug binding domains, MBPhtopo$^{1-266}$, contains the ATP binding pocket, we next tested whether ATP competes for the binding of etoposide to the holoenzyme. We find that the amount of

(^{3}H)VP16 bound to wild-type yeast topoII drops by 75% in the presence of 1.0 mM ATP (Figure 3A). A similar result is obtained with yeast topoII carrying a Tyr to Phe mutation at the active site (ytop2Y$_{782}$F, numbering according to SwissProt), indicating that the active site hydroxyl group is not required either for the efficient binding of VP16 or for ATP competition. Although the concentration of ATP required for displacement is high, it is consistent with the K_m values of 0.3 and 0.47 mM calculated for ATPase activity of yeast and human topoII in the absence of DNA (*50*, *51*). Importantly, however, equivalent concentrations of ATP do not displace VP16 from the B′A′ fusion protein MBPhtopo$^{430-1214}$ (Figure 3A). Antagonism between ATP and drug binding was further confirmed by showing that increasing amounts of VP16 can displace (α^{32}P)ATP from intact yeast topoII (Figure 3B). In addition, a 40-fold molar excess of VP16 reduces to 50% the covalent labeling of either yeast holoenzyme or MBPhtopo$^{1-266}$ with the photoaffinity cross-linker azido(α^{32}P)ATP (Figure 3E). In this case, the incomplete displacement either may be due to the rapid and irreversible character of light-induced cross-linking events (see *52*) or may indicate that the two compounds do not directly compete for the same binding site.

The drug binding specificity of both the full-length yeast topoII and MBPhtopo$^{1-426}$ was examined through competition with unlabeled VP16, VM26, *m*-AMSA, *o*-AMSA, and ATP. VP16 and VM26 are related epipodophyllotoxins, and *m*-AMSA is an efficient intercalating inhibitor, while *o*-AMSA is a related, but inactive compound. As shown in Figure 3C, 200 μM samples of VP16 or VM26 or 1 mM ATP reduces by 75% the amount of (^{3}H)VP16 recovered with the full-length protein. Similar results are obtained with MBPhtopo$^{1-426}$ for VP16 or ATP, with a slightly reduced displacement by VM26 and an increased effect for *m*-AMSA (Figure 3D). *o*-AMSA competes with VP16 weakly when MBPhtopo$^{1-426}$ is used, and fails to displace etoposide significantly from the yeast holoenzyme, consistent with the fact that *o*-AMSA is a poor topoII inhibitor.

To estimate the relative affinity of potential drug binding sites, the assays presented here have been performed in the absence of DNA. It is clear, however, that the binding of DNA and the efficiency of ATP hydrolysis may influence the inhibitor−enzyme complex that is formed in vivo (*53*−*55*). Since DNA was found to interfere with our spin column assay, we next asked whether the ATPase activity of purified yeast topoII is modified by the addition of VP16. As reported by Hammonds and Maxwell (*56*) and more recently by Morris and Lindsley (*55*), we find that increasing concentrations of VP16 inhibit the DNA-stimulated ATP hydrolysis of the holoenzyme by about 50% (Figure 3F). The latter authors propose that in the presence of the drug, inhibition of ATPase activity occurs after hydrolysis of the first ATP molecule and before release of the second ADP, resulting in this partial inhibition. The two ligands are suggested to bind in a hyperbolic noncompetitive manner, in which, unlike normal noncompetitive binding, the presence of one ligand indirectly impedes efficient binding of the other (*55*).

Modeling of the ATP Binding Pocket and Docking of VP16. Based on the unexpected antagonism between ATP and VP16 for binding the topoII N-terminus, we next examined how the two ligands might fit into this small, well-structured domain. As a basis for molecular modeling, we

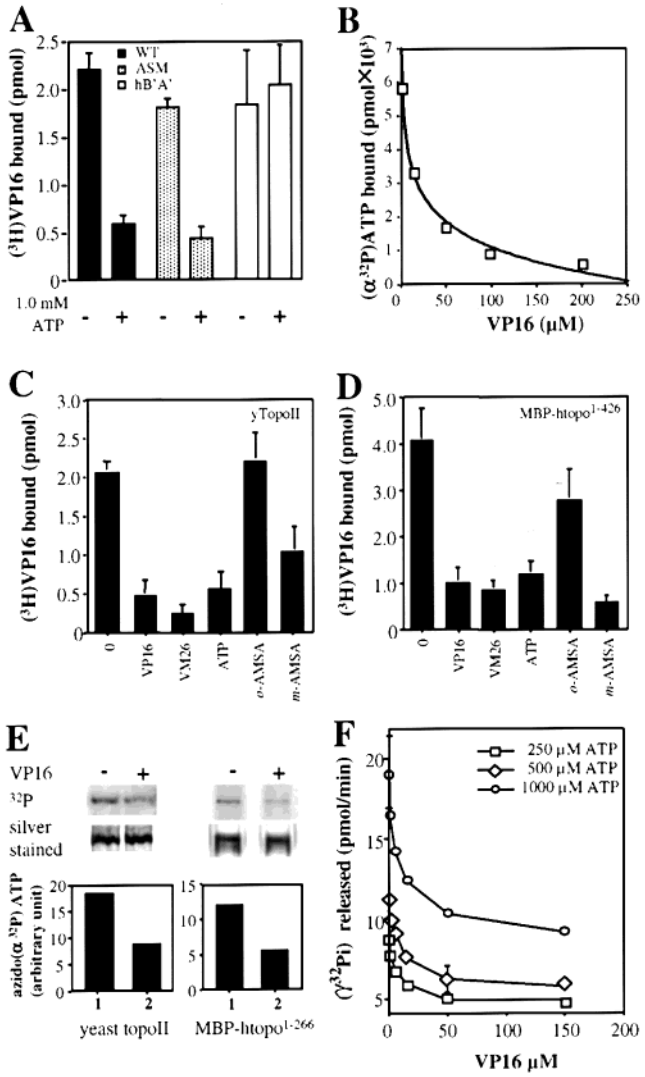

FIGURE 3: ATP impairs VP16 binding. (A) (^{3}H)VP16 binding is antagonized by ATP for wild-type (WT) yeast topoII and an active site mutant (ASM ytopoIIY$_{782}$F). The assay is performed as in Figure 1A using (^{3}H)VP16 (10^3 pmol, 1.0 μCi) with 2.5 pmol (dimer) of either form of yeast topoII or 12 pmol of MBPhtopo$^{430-1214}$, without or with 1.0 mM ATP (5×10^4 pmol). Results are plotted after subtraction of the radioactivity recovered in the absence of topoII or in the presence of MBP−CK2β when MBPhtopo$^{430-1214}$ is used. (B) Displacement of (α^{32}P)ATP by VP16. (α^{32}P)ATP (5 pmol, 2.0 μCi) is incubated with 2.5 pmol of yeast topoII (dimer) as in panel A with increasing concentrations of VP16. Results are plotted after the subtraction of the control values. (C) Drug binding specificity. Yeast topoII (2.5 pmol, dimer) is incubated in duplicate with (^{3}H)VP16 (1.0 μCi) as in (A) without or with 200 μM VP16, VM26, *o*-AMSA, *m*-AMSA, or 1.0 mM ATP. Data are plotted after subtraction of control values. (D) Drug binding specificity performed as described in (C) but with MBPhtopo$^{1-426}$ (10 pmol of monomer). (E) Photolabeling of yeast topoII and MBPhtopo$^{1-266}$ with azido(α^{32}P)ATP is reduced in the presence of VP16. Purified yeast topoII (15 pmol, left panel) and MBPhtopo$^{1-266}$ (30 pmol, right panel) are incubated with azido-(α^{32}P)ATP (200 pmol; 4 μCi) in the absence or presence of 200 μM VP16 (8×10^3 pmol) in the dark for 20 min, and then irradiated at 330 nm for 10 min. After SDS−PAGE and silver staining, ^{32}P is quantified (Phosphorimager, Molecular Dynamics) and normalized to protein amount. (F) ATPase activity of yeast topoII. Purified yeast topoII (0.3 pmol) is incubated in the absence or in the presence of increasing concentrations of VP16 with (γ^{32}P)ATP (1.0 mCi) and 250, 500, or 1.0 mM ATP at 37 °C. After 30 min, released (γ^{32}P)P$_i$ is recovered, and the amount of radioactivity is analyzed by scintillation liquid counting as described under Experimental Procedures. Assays are performed in duplicate.

Table 1: Geometry of Hydrogen Bonds in the VP16−Topoisomerase II Complex[a]

protein donor groups (DH)	VP16 acceptor groups (A)	distance (Å) H−A	angle (deg) HD−A
Asn_{91} NH	O11	2.1	12
Asn_{95} NH	O13	2.0	30
Asn_{120} NH	O12	2.0	26
Lys_{123}	O6	2.1	32
Gly_{124} NH	O7	2.2	30
Ser_{149} OH	O5	2.0	35
Arg_{184} NH	O3	2.1	31

[a] Using the molecular substitution of htopoIIα sequence into the crystal structure of GyrB [Lewis et al. (*16*)], we have docked etoposide in the ATP binding pocket (see Figure 4). We list here the parameters of the hydrogen bonds that would stabilize the most energetically favorable interaction.

used the GyrB ATPase domain, which has been cocrystallized with both ADPNP and novobiocin (*15*, *16*). The structures indicate that novobiocin sits in the upper part of the ATP binding pocket, overlapping partially with ATP, which binds at the bottom of this same cleft (Figure 4A,D). The hydrogen bonds that stabilize novobiocin within the pocket involve primarily the antibiotic's sugar groups, and the amino acid residues Asn_{46}, Asp_{73}, Ile_{78}, Arg_{136}, and Thr_{165}. To see if VP16 might also fit in the ATP binding pocket of GyrB, we performed a molecular docking analysis. First VP16 was built (program TURBO−FRODO, *37*), and its most stable conformation was analyzed by molecular dynamics simulation and energy minimization (*38*, *39*). Due to covalent and steric constraints, VP16 preserves a cross-shaped structure with one axis made of the sugar and the 4-hydroxy-3,5-dimethoxyphenyl group and the other axis formed by the four-ringed moiety (Figure 4G). The planar shape of the ringed moiety is conserved among many topoII inhibitors (data not shown). Docking VP16 in the ATP binding pocket of GyrB revealed a good fit, although consistent with its lower affinity, the fit of etoposide is energetically less favorable than that of novobiocin (data not shown).

The extensive homology between GyrB and htopoIIα N-termini allowed a homology-based modeling of the eukaryotic ATP binding domain, and the subsequent molecular docking of VP16 into this polypeptide pocket. Energy minimization calculations indicate values for the VP16/htopoII ATPase domain complex that are 2 kcal/mol lower than those for the VP16/GyrB complex. Figures 4B and 4E show our proposal for the 3D structure of the htopoIIα ATPase domain with both VP16 (in yellow) and ATP (in green) bound. The amino acids putatively involved in the binding of VP16 are Asn_{91}, Asn_{95}, Asn_{120}, Lys_{123}, Gly_{124}, Ser_{149}, and Arg_{184} (Figure 4B,E), which could collectively contribute seven stabilizing hydrogen bonds to the drug (see Table 1 and Figure 4H). As with gyrase, the polycyclic central domain of VP16 fits in the trough which is defined by Lys_{123}, Pro_{126}, Ile_{141}, Ser_{149}, and Glu_{155} residues (Figure 4B), allowing us to predict mutations that might weaken this interaction (see Figure 4C,F and below). The binding of etoposide is thus predicted to impede but not eliminate ATP binding.

Drug Binding Activity of Mutant HtopoIIα N-Terminal Domains. To test relevance of the modeling data, we introduced point mutations into the ATP binding domain of htopoIIα (aa 1−440), changing residues that were predicted to participate in drug binding. Two types of point mutations were made. First, Val_{137} and Glu_{155} were replaced with Trp and Phe, respectively, the prediction being that the bulkier side chains of these latter residues would interfere with the central polycyclic moiety of VP16 (Figure 4C,F, mutations in pink). Second, Lys_{123} was exchanged for alanine to eliminate the hydrogen bond between the nitrogen of Lys_{123} and the O6 atom of VP16 (Figure 4H). Finally, as a general control for the validity of the molecular substitution technique and the predicted structure, Gly_{164} of the Walker motif was replaced with Val (Figure 4F, in pink). If our modeling was correct, the Gly_{164}Val mutation should affect ATP, but not drug, interaction.

The wild-type (WT) and mutated MBPhtopo$^{1-440}$ domains were expressed in *E. coli* and purified to near-homogeneity (Figure 2B,C, lanes 4−7). To compare their drug binding efficiencies, equivalent amounts of each protein were incubated with (^{3}H)VP16, and the complexes were analyzed by the gel filtration method described above. A low background, reflecting the nonspecific interaction of drug with MBP−CK2β, was subtracted from all values. Consistent with our predictions, Figure 5A shows that the amount of VP16 recovered with the V_{137}W, E_{155}F, and K_{123}A domains corresponds maximally to 40% of that bound to the WT domain, whereas the Walker motif mutation (G_{164}V) binds VP16 as efficiently as the WT protein. A stained SDS gel confirms that the stabilities and recoveries of the mutant and WT domains are equal (inset, Figure 5A). Introduction of the E_{155}F and K_{123}A mutations into the human topoIIα holoenzyme produces functional enzymes in yeast, confirming that the mutations do not grossly affect folding of the protein (data not shown).

As a further control that the mutated domains are properly folded, we monitored their ability to bind ATP. Equivalent amounts of each fusion protein were incubated with (α^{32}P)-ATP and the complexes were analyzed as described above. The mutated domains V_{137}W, E_{155}F, and K_{123}A all bind ATP as well or slightly better than the WT domain (Figure 5B), suggesting that the ATP binding pocket is correctly folded. The increased binding may reflect a lower off-rate due to a higher hydrophobicity within the cleft. Replacement of the Walker motif Gly_{164} with Val reduces ATP binding by 60%, as expected, but has no major effect on etoposide interaction. Taken together, these results support the hypothesis that the residues Val_{137}, Glu_{155}, and Lys_{123} help stabilize etoposide without being directly implicated in the correct coordination of ATP. Val_{164}, on the other hand, which sits at the bottom of the ATP binding pocket, lowers the binding efficiency of ATP.

The change in apparent K_d for the WT and mutant domains was determined as described above, using MBPhtopo$^{1-440}$ and MBPhtopo$^{1-440}V_{137}$W. In agreement with Figure 5A, half as much (^{3}H)VP16 binds the mutated protein as binds the WT protein in the absence of unlabeled VP16. Increasing concentrations of competitor displace the radioactive form from both WT and mutated domains, reaching a plateau at 150 μM etoposide (Figure 5C). From Scatchard plot analysis, we estimate a 4-fold change in the apparent K_d (from 28 to 106 μM). The stoichiometry of drug to monomer remains unaltered, with 0.9 and 1.2 drug molecules bound per

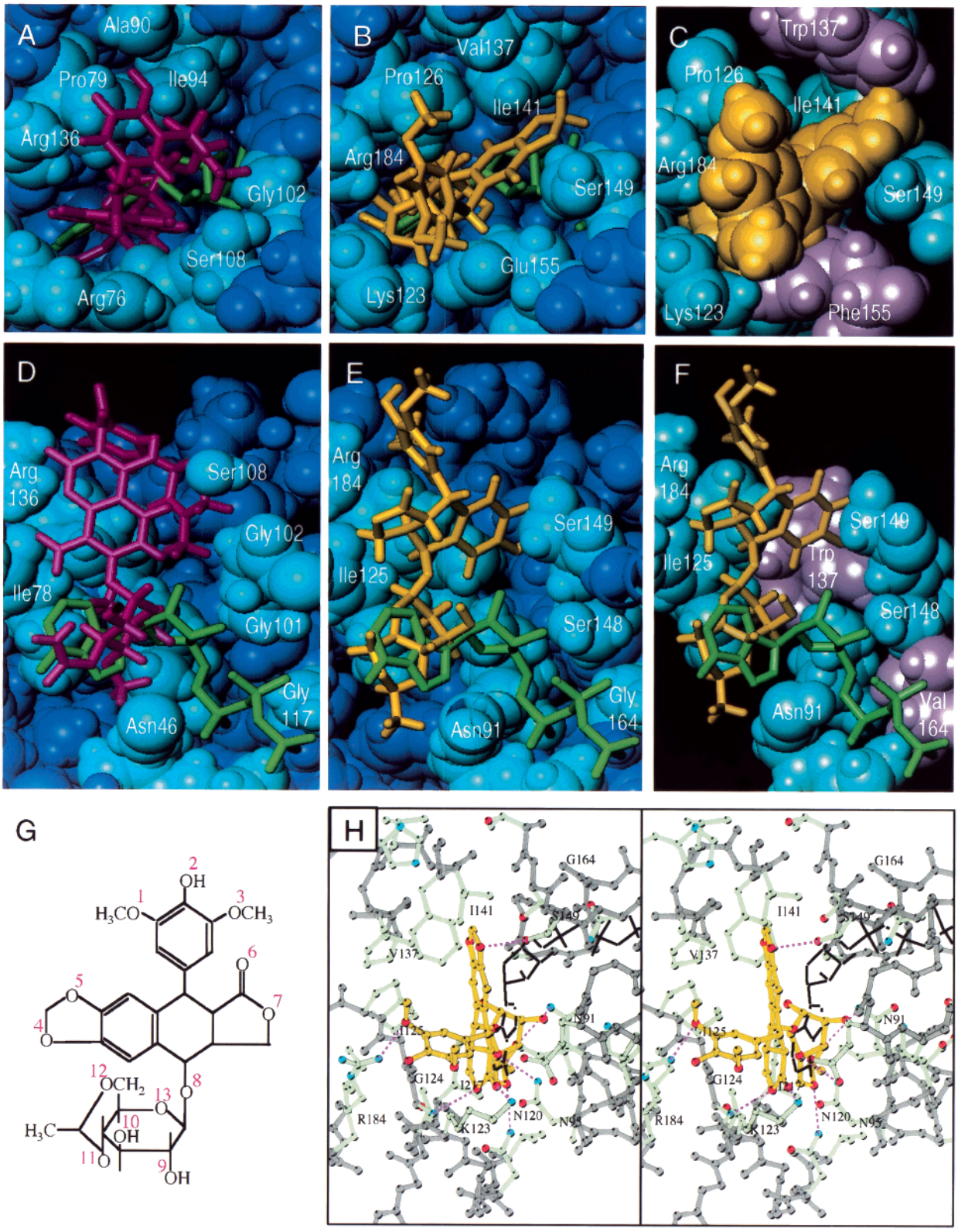

FIGURE 4: Representation of the drug binding site in the ATP binding pockets of DNA gyrase and htopoIIα. (A) The crystal structure of the GyrB/novobiocin complex [aa 1−220; Lewis et al. (*16*)] is viewed from the top of the pocket and from the side in (D). Residues implicated in antibiotic, drug, and ATP binding are in light blue. Novobiocin is in red, and ATP is in green. (B) The modeled VP16/htopoIIα complex is viewed from the top of the pocket and from the side in (E). VP16 is in yellow. (C) Modeled VP16/htopoIIα complex carrying the point mutations Trp_{137} and Phe_{155} in pink and VP16 in space-filling mode (top view). (F) As panel C, except that the mutation Gly_{164}→Val is shown. VP16 is in yellow and ATP in green. Figures are generated with the program TURBO−FRODO (*37*). (G) Chemical structure of etoposide (VP16). Oxygen atoms including those relevant for the hydrogen bonds listed in Table 1 are numbered in red. (H) Stereoview of the modeled VP16/htopoIIα complex, from the top of the pocket. The backbone chain of topoIIα is in gray, amino acid side chains are in green, VP16 is in yellow, and ATP is in black. Oxygen atoms are in red, and nitrogen atoms are in blue. Dashed red lines indicate hydrogen bonds between VP16 and topoIIα, as summarized in Table 1. This image is generated with the program MOLSCRIPT (*41*).

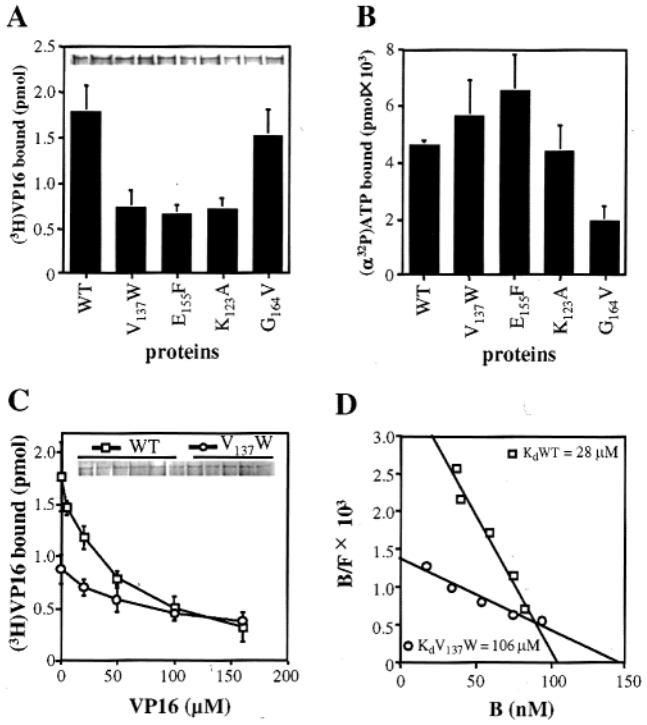

FIGURE 5: Drug binding activity of the mutated and the wild-type N-terminal domain of htopoIIα. (A) Equivalent amounts (5 pmol) of purified MBP-fusion proteins carrying wild-type (WT) or mutated forms of htopoIIα$^{1-440}$ ($V_{137}W$, $E_{155}F$, $K_{123}A$, or $G_{164}V$) are incubated in duplicate with (^{3}H)VP16 (10^3 pmol, 1.0 μCi) as described in Figure 1A. Results are normalized to protein recovery (>90%), and are plotted after subtraction of MBP−CK2β bound (≤0.8 pmol). For each assay, 1/10 of the flow-through is analyzed by gel electrophoresis, silver staining, and quantitative scanning (inset). (B) ATP binding activity of the WT and mutated htopoIIα N-terminal domains used in panel A. Assays are performed in duplicate and are normalized as described in (A), but using (α^{32}P)-ATP (5 pmol, 2.0 mCi) in place of (^{3}H)VP16. (C) Equivalent amounts (6 pmol) of WT and mutated $V_{137}W$ N-terminal domains are incubated in duplicate with (^{3}H)VP16 (10^3 pmol, 1.0 μCi) as above with increasing amounts of unlabeled VP16. Data are plotted after subtraction of the MBP−CK2β background (≤0.9 pmol), and after normalization to protein recovery. For the duplicate points, 1/20 of the recovered flow-through is pooled and analyzed as in (A) (gel shown in inset). (D) Scatchard plot of data in panel C. The reciprocals of the slopes give the apparent K_d values of 28 and 106 μM for the WT and mutated domains, respectively. The binding stoichiometry is 0.9 VP16 molecule per WT N-terminal domain and 1.2 VP16 molecules per $V_{137}W$ domain.

monomer for the WT and mutant proteins, respectively (Figure 5D).

DISCUSSION

In view of the widespread use of topoII inhibitors in chemotherapy, and the frequency with which drug resistance occurs after extended treatment, it is important to both basic and biomedical research to understand how topoII inhibitors function. Indirect evidence has led to the notion that the catalytic site of topoisomerase II plays a key role in the drug/protein interaction. First, topoII inhibitors were shown to exhibit a significant nucleotide specificity at the level of the DNA cleavage site (*53*, *57*, *58*). Second, a derivative of amsacrine was covalently cross-linked on nucleotides adjacent to the topoII-mediated cleavage site in DNA (*59*). Third, it was shown that the central catalytic core of topoII is sufficient to form a stable complex with a DNA double-strand break in response to bisdioxopiperazine or epipodophyllotoxins (*48*).

More recently, however, the N-terminal domain of topoII was also implicated in the drug-mediated inhibition of the enzyme's catalytic activity. Epipodophyllotoxins were shown to inhibit topoII activity after hydrolysis of the first ATP molecule and before releasing the second (*55*), and the N-terminal ATPase domain of yeast topoII was proposed to bind the bisdioxopiperazine class of topoII inhibitors (*49*). Consistent with this is the characterization of an ICRF-187 resistance phenotype in human small cell lung cancer cells which carry a $R_{162}Q$ mutation in the Walker A motif of the topoIIα ATP binding pocket (*60*). To better understand the interaction between etoposide and topoII at a molecular level, we have characterized drug binding in vitro, modeled the protein and ligand interaction, and created appropriate mutations to test the predicted fit. As summarized below, we find that mutations in the upper part of the ATP binding cleft, which themselves do not interfere with ATP binding, significantly alter interaction with etoposide in vitro.

VP16 Has Two Binding Sites in TopoII. Using a direct drug binding assay, we identify two subdomains of htopoIIα that are sufficient to bind the nonintercalating inhibitor etoposide (VP16) independently, in the absence of DNA. The apparent K_d for the 266 aa N-terminal fragment is close to that measured for the yeast and human holoenzymes by the same technique ($K_d \approx 20$ μM), while the core domain (aa 430−1214) binds with even higher affinity ($K_d \approx 9$ μM). The K_m of VP16 for trapping *Drosophila* topoII in a covalent complex with DNA was reported to range from 3.5 to 42 μM (*10*). These values are comparable to the ones obtained in our spin column assay (20, 27, 20, and 9 μM), even though the assay used by Burden et al. (*10*) is performed in the presence of DNA substrate. Consistent with our observations, these authors present evidence that etoposide binds the holoenzyme directly, prior to binding DNA. Similarly, Kingma et al. (*61*) have estimated a K_d value of 5 μM for the interaction of VP16 with yeast topoII using a glass fiber filter assay, again in the absence of DNA.

We further show that the binding of etoposide to the core domain is not sensitive to ATP, while association with both the N-terminal domain and the holoenzyme is antagonized by high concentrations of ATP (1 mM). This is unlikely to be due to the hydrolysis of this nucleotide during incubation, since yeast topoII has very low ATPase activity at room temperature in the absence of DNA (data not shown; *50*). The concentration of ATP required for competition is consistent with the K_m value for ATP determined for the ATPase activity of topoII in the absence of DNA (0.3 mM for the yeast enzyme and 0.47 mM for the human protein; *50*, *51*).

Mutation of the ATP Binding Pocket Affects Etoposide Binding. The autonomy of the ATP binding domain for drug interaction led us to perform molecular modeling of the human N-terminal ATPase domain, which could be based reliably on structural information from cocrystals of the GyrB N-terminal domain with novobiocin and with ATP (*16*). Docking experiments suggest that VP16 fits readily into the ATP binding cleft of both gyrase and htopoIIα, and like novobiocin, the drug's sugar group overlaps only partially with the adenine ring moiety of the nucleotide triphosphate. Consistent with the prediction that Gly_{164} will contact ATP,

but not the drug, we found that substitution of Val for Gly_{164} interferes with the binding of ATP, but not of VP16.

The molecular modeling studies predicted that specific amino acids in the ATP binding pocket could be involved in drug interaction, and subsequent mutagenesis is consistent with these predictions. Two of the point mutations introduce bulky, hydrophobic side chains into the predicted ligand binding site, and a third eliminates one of the stabilizing hydrogen bonds. In each case, the efficiency of drug interaction drops, although ATP is still efficiently bound. This latter result suggests that the MBP fusions are correctly folded, despite the fact that they are inactive for ATP hydrolysis. This inactivity may reflect their lack of dimerization, a step that is apparently required for both ATPase and DNA double-strand cleavage activities (*51*, *62*). For the $V_{137}W$ mutation, the apparent dissociation constant for etoposide shows a 4-fold increase over that of the wild-type N-terminal domain. This value is close to the variation observed in the affinity of VP16, ellipticine (*61*, *63*), and coumarins (*64*) for mutant forms of yeast topoII and gyrase, respectively. We have identified a drug binding activity in the N-terminal ATPase domain of topoII, in addition to the high-affinity binding site in the core domain. This second DNA-independent drug binding site in the N-terminus of topoisomerase II provides a mechanism by which truncated forms of topoII can compete for inhibitors even when they are not nuclear-localized (*65*, *66*). Indeed, recent results show that the expression of the wild-type N-terminal domain of human topoIIα, in yeast, enhances drug resistance in vivo (N. Vilain, S. M. Gasser, and D. Leroy, manuscript in preparation).

Two Potential Models for TopoII−Drug Interaction. Our results suggest that etoposide binds at two distinct sites within htopoIIα in the absence of DNA. Each binding site has different characteristics: one is sensitive to ATP concentrations (N-term, Figure 3D), while the binding to the core domain can be competed by phenylalanine (data not shown). Since we calculate a 1:1 binding ratio for VP16 to topoII monomer, the two sites may bind VP16 in a mutually exclusive manner or may cooperate to form a single binding pocket in the holoenzyme. Data from other laboratories suggest that the drug binding site in the core domain is not only critical but also sufficient to stabilize the DNA−topoII complex in vitro (*54*, *59*). On the other hand, mutations in the N-terminal ATPase domain have been shown to affect drug sensitivity in vivo (*60*). Moreover, the topoII inhibitor ICRF-193 was found to bind the isolated N-terminal domain of yeast topoII in vitro (*49*).

We propose two models for drug−enzyme interaction, as portrayed in Figure 6. In the first, we propose that the N-terminal and the core domain binding sites are both directly involved in the tertiary complex formed between DNA, topoII, and the drug. The two sites may participate in the creation of a unique drug binding pocket. In such a situation, alteration of one or the other site, by appropriate amino acid changes specifically designed to impair drug binding, should confer a drug resistance phenotype to the cells expressing these mutated forms of topoII. Alternatively, the N-terminal site may not be implicated in the stabilization of the cleavable complex, and may only be available to bind etoposide in the absence of DNA or when ATP is limiting (Figure 6B). Nonetheless, this site could modulate the binding

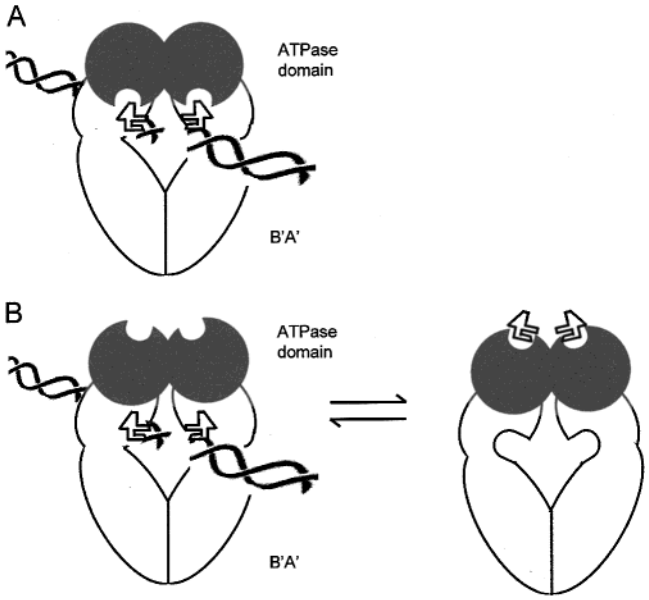

FIGURE 6: Models for etoposide binding to eukaryotic topoisomerase II. (A) Based on the studies described here, we propose that each monomer of topoII carries two physically distinct etoposide binding sites, one in the N-terminal ATPase domain and the other in the catalytic core domain. The two sites may cooperate to form a single drug binding site in the holoenzyme, which stabilizes the cleavable complex between enzyme and DNA. If one or the other site is altered by mutagenesis, a drug-resistant enzyme would be expected to result from the modification. (B) Alternatively, the drug binding site in the catalytic core domain may be the only one which can stabilize the DNA double-strand break. In such a situation, the N-terminal drug binding site could be considered as a negative regulator that would compete with the core domain for the drug. This could be particularly relevant in drug-limiting conditions that may occur in yeast (*65*). If mutations are introduced into the N-terminal domain, such that it binds etoposide less efficiently, more antitumor agent may become available to the catalytic core domain, resulting in enhanced drug sensitivity of the mutant enzyme.

of the drug to the core domain in limiting concentrations of antitumor agents, by competing for the drug. In this case, any detrimental amino acid changes that would affect etoposide binding to the N-terminal domain should render the drug more available for the DNA-modifying B′A′ domain, leading to a hypersensitivity phenotype.

In summary, a gel filtration based interaction assay has revealed two potential etoposide binding sites within htopoIIα, one in the B′A′ core and one within the N-terminal ATPase domain. Site-directed mutagenesis of residues facing the ATP binding pocket has been shown to lower the affinity of the purified recombinant subdomains for the inhibitor. It is not known whether the two sites cooperate or compete for drug binding in the holoenzyme, but the possibility of an N-terminal drug binding site helps explain how this domain can be implicated in topoII-mediated drug resistance in vivo.

ACKNOWLEDGMENT

We thank A. Maxwell for crystallographic coordinates, Y. Pommier for drugs, A. Soltermann and A. Ernst for plasmids, C. Austin for purified human topoisomerase IIα, J. Lingner and members of the Gasser laboratory for carefully reading the manuscript, and U. K. Laemmli for the active site mutant plasmid and helpful discussions. We thank P.

Dubied for help with the figures. D.L. thanks the ARC, Rhône-Alpes Exchange Program, and EMBO for fellowships, and we thank ISREC for support of A.V.K.

REFERENCES

1. Dinardo, S., Voelkel, K., and Sternglanz, R. (1984) *Proc. Natl. Acad. Sci. U.S.A. 81*, 2616−2620.
2. Holm, C., Goto, T., Wang, J. C., and Botstein, D. (1985) *Cell 41*, 553−563.
3. Uemura, T., and Yanagida, M. (1984) *EMBO J. 3*, 1737−1744.
4. Uemura, T., Ohkura, H., Adachi, Y., Morino, K., Shiozaki, K., and Yanagida, M. (1987) *Cell 50*, 917−925.
5. Adachi, Y., Luke, M., and Laemmli, U. K. (1991) *Cell 64*, 137−148.
6. D'Arpa, P., and Liu, L. F. (1989) *Biochim. Biophys. Acta 989* (2), 163−177.
7. Corbett, A. H., and Osheroff, N. (1993) *Chem. Res. Toxicol. 6*, 584−597.
8. Pommier, Y. (1997) DNA topoisomerase II inhibitors. in *Cancer Therapeutics: Experimental and Clinical Agents* (Teicher, B., Ed.) pp 153−173, Humana Press Inc., Totowa, NJ.
9. Chow, K. C., Macdonald, T. L., and Ross, W. E. (1988) *Mol. Pharmacol. 34*, 467−473.
10. Burden, D. A., Kingma, P. S., Froelich-Ammon, S. J., Bjornsti, M.-A., Patchan, M. W., Thompson, R. B., and Osheroff, N. (1996) *J. Biol. Chem. 271*, 29238−29244.
11. Sugino, A., Higgins, N. P., Brown, P. O., Peebles, C. L., and Cozzarelli, N. R. (1978) *Proc. Natl. Acad. Sci. U.S.A. 75*, 4838−4842.
12. Sugino, A., and Cozzarelli, N. R. (1980) *J. Biol. Chem. 255*, 6299−6306.
13. Staudenbauer, W. L., and Orr, E. (1981) *Nucleic Acids Res. 9*, 3589−3603.
14. Nakada, N., Gmuender, H., Hirata, T., and Arisawa, M. (1994) *Antimicrob. Agents Chemother. 38*, 1966−1973.
15. Wigley, D. B., Davies, G. J., Dodson, E. J., Maxwell, A., and Dodson, G. (1991) *Nature 351*, 624−629.
16. Lewis, R. J., Singh, O. M., Smith, C. V., Skarzynski, T., Maxwell, A., Wonacott, A. J., and Wigley, D. B. (1996) *EMBO J. 15*, 1412−1420.
17. Caron, P. R., and Wang, J. C. (1993) *International Symposium on DNA topoisomerases in Chemotherapy*, Nagoya, Japan, CRC Press, Inc., Boca Raton, FL, pp 1−18.
18. Hinds, M., Deisseroth, K., Mayes, J., Altschuler, E., Jansen, R., Ledley, F. D., and Zwelling, L. A. (1991) *Cancer Res. 51*, 4729−4731.
19. Lee, M. S., Wang, J. C., and Beran, M. (1992) *J. Mol. Biol. 223*, 837−843.
20. Campain, J. A., Gottesman, M. M., and Pastan, I. (1994) *Biochemistry 33*, 11327−11332.
21. Freudenreich, C. H., Chang, C., and Kreuzer, K. N. (1998) *Cancer Res. 58*, 1260−1267.
22. Sabourin, M., Byl, J. A., Hannah, S. E., Nitiss, J. L., and Osheroff, N. (1998) *J. Biol. Chem. 273*, 29086−29092.
23. Strumberg, D., Nitiss, J. L., Rose, A., Nicklaus, M. C., and Pommier, Y. (1999b) *J. Biol. Chem. 274*, 7292−7301.
24. Vassetzky, Y. S., Alghisi, G.-C., and Gasser, S. M. (1995) *BioEssays 17*, 767−774.
25. Nitiss, J. L., and Beck, W. T. (1996) *Eur. J. Cancer 32A*, 958−966.
26. Watt, P. M., and Hickson, I. D. (1994) *Biochem. J. 303*, 681−695.
27. Beck, W. T., Danks, M. K., Wolverton, J. S., Kim, R., and Chen, M. (1993) *Adv. Enzyme Regul. 33*, 113−127.
28. Larsen, A. K., and Skladanowski, A. (1998) *Biochim. Biophys. Acta 1400*, 257−274.
29. Cardenas, M. E., Walter, R., Hanna, D. E., and Gasser, S. M. (1993) *J. Cell Sci. 104*, 533−543.
30. Cornarotti, M., Tinelli, S., Willmore, E., Zunino, F., Fisher, L. M., Austin, C. A., and Capranico, G. (1996) *Mol. Pharmacol. 50*, 1463−1471.
31. Tsai-Pflugfelder, M., Liu, L. F., Liu, A. A., Tewey, K. M., Whang-Peng, J., Knutsen, T., Huebner, K., Croce, C. M., and Wang, J. C. (1988) *Proc. Natl. Acad. Sci. U.S.A. 85*, 7177−7181.
32. Guan, C., Li, P., Riggs, P. D., and Inouye, H. (1988) *Gene (Amsterdam) 67*, 21−30.
33. Soltermann, A., Ernst, A., Leroy, D., Stahel, R., and Gasser, S. M. (1999) *Exp. Cell Res. 248*, 308−319.
34. Cormack, B. (1991) Mutagenesis by the polymerase chain reaction. in *Current Protocols in Molecular Biology* (Ausubel, F. M., Brent, R., Kingston, R. E., Moore, D. D., Seidman, J. G., Smith, J. A., and Struhl, K., Eds.) pp 8.5.1−8.5.9, Greene Publishing Associates and Wiley-Interscience, New York.
35. Penefsky, H. S. (1977) *J. Biol. Chem. 252*, 2891−2899.
36. Leroy, D., Hériché, J.-K., Filhol, O., Chambaz, E. M., and Cochet, C. (1997b) *J. Biol. Chem. 272*, 20820−20827.
37. Roussel, A., and Cambillan, C. (1989) *Silicon Graphics geometry partner directory*, pp 77−78, Silicon Graphics, Mountain View, CA.
38. Brooks, B. R., Bruccoleri, R. E., Olafson, B. D., States, D. J., Swaminathan, S., and Karplus, M. (1983) *J. Comput. Chem. 4*, 187−217.
39. Brunger, A. T., Kuriyan, J., and Karplus, M. (1987) *Science 235*, 458−460.
40. Abagyan, R., Totrov, M., and Kuznetsov, D. (1994) *J. Comput. Chem. 15*, 488−506.
41. Kraulis, P. J. (1991) *J. Appl. Crystallogr. 24*, 946−950.
42. Laemmli, U. K. (1970) *Nature 227*, 680−685.
43. Zeeberg, B., and Caplow, M. (1979) *Biochemistry 18*, 3880−3886.
44. Kitajima, S., and Uyeda, K. (1983) *J. Biol. Chem*, *258*, 7352−7357.
45. Leroy, D., Filhol, O., Delcros, J.-G., Pares, S., Chambaz, E. M., and Cochet, C. (1997a) *Biochemistry 36*, 1242−1250.
46. Jensen, S., Andersen, A. H., Kjeldsen, E., Biersack, H., Olsen, E. H. N., Andersen, T. B., Westergaard, O., and Jakobsen, B. K. (1996) *Mol. Cell. Biol. 16*, 3866−3877.
47. Berger, J. M., Gamblin, S. J., Harrison, S. C., and Wang, J. C. (1996) *Nature 379*, 225−232.
48. Chang, S., Hu, T., and Hsieh, T.-S. (1998) *J. Biol. Chem. 273*, 19822−19828.
49. Olland, S., and Wang, J. C. (1999) *J. Biol. Chem. 274*, 21688−21694.
50. Lindsley, J. E., and Wang, J. C. (1993) *J. Biol. Chem. 268*, 8096−8104.
51. Gardiner, L. P., Roper, D. I., Hammonds, T. R., and Maxwell, A. (1998) *Biochemistry 37*, 16997−17004.
52. Pomerantz, A. H., Rudolph, S. A., Haley, B. E., and Greengard, P. (1975) *Biochemistry 14*, 3858−3862.
53. Burden, D. A., and Osheroff, N. (1998) *Biochim. Biophys. Acta 1400*, 139−154.
54. Strumberg, D., Nitiss, J. L., Dong, J., Kohn, K. W., and Pommier, Y. (1999a) *J. Biol. Chem. 274*, 28246−28255.
55. Morris, S. J., and Lindsley, J. E. (1999) *J. Biol. Chem. 274*, 30690−30696.
56. Hammonds, T. R., and Maxwell, A. (1997) *J. Biol. Chem. 272*, 32696−32703.
57. Kingma, P., and Osheroff, N. (1997) *J. Biol. Chem. 272*, 1148−1155.
58. Capranico, G., and Binaschi, M. (1998) *Biochim. Biophys. Acta 1400*, 185−194.
59. Freudenreich, C. H., and Kreuzer, K. N. (1994) *Proc. Natl. Acad. Sci. U.S.A. 91*, 11007−11011.
60. Wessel, I., Jensen, L. H., Jensen, P. B., Falck, J., Rose, A., Roerth, M., Nitiss, J. L., and Sehested, M. (1999) *Cancer Res. 59*, 3442−3450.
61. Kingma, P. S., Burden, D. A., and Osheroff, N. (1999) *Biochemistry 38*, 3457−3461.
62. Ali, J. A., Jackson, A. P., Howells, A. J., and Maxwell, A. (1993) *Biochemistry 32*, 2717−2724.
63. Froelich-Ammon, S. J., Burden, D. A., Patchan, M. W., Elsea, S. H., Thompson, R. B., and Osheroff, N. (1995) *J. Biol. Chem. 270*, 28018−28021.

64. Kampranis, S. C., Gormley, N. A., Tranter, R., Orphanides, G., and Maxwell, A. (1999) *Biochemistry 38*, 1967−1976.

65. Vassetzky, Y. S., Alghisi, G. C., Roberts, E., and Gasser, S. M. (1996) *Br. J. Cancer 73*, 1201−1209.

66. Mirski, S. E., Sparks, K. E., Yu, Q., Lang, A. J., Jain, N., Campling, B. G., and Cole, S. P. (2000) *Int. J. Cancer 85*, 534−539.

BI0019141